Volume 34 Number 1
2023

Power output characterisation of thermoelectric generator units coupled to inverted box rib sheeting

Momina Malik, **Mark Gilpin**, **Bruce Graham**
Department of Mechanical Engineering, Durban University of Technology, Durban, South Africa

Abstract
There is a global need for clean and renewable energy sources. This study investigated thermoelectric generators (TEGs) as a possible method for harvesting solar power. The TEG prototype tested here consisted of two equally sized pieces of roof sheeting, with one side exposed to a light source and the other side shaded. Experiments were carried out with the necessary testing components to investigate the effects that two variables have on the amount of power generated: first, the colour of metal inverted box rib (IBR) sheeting and, second, the ideal electrical arrangement for scalability of Peltier tiles for maximum power output. Black-coated sheets generated maximum power (Pmax) output of the TEGs. The TEGs in series configuration generated the highest Pmax when located closest to the light source. The conclusion from the experiment is that TEGs are a potential method of harvesting solar energy on IBR sheeting, specifically in a vertical position. However, applications of different orientations and geographical locations require further investigation, including into the use of TEGs on IBR sheeting for harvesting solar energy on a larger scale.

Keywords: IV curve generation method; maximum power output; Peltier tiles; Pmax; temperature gradient

Journal of Energy in Southern Africa 34(1),1–14
DOI: https://dx.doi.org/10.17159/2413-3051/2023/v34i1a17264
Published by the University of Cape Town ISSN: 2413-3051 https://journals.assaf.org.za/jesa

Sponsored by the Department of Science and Innovation

Corresponding author: E-mail: momina270@gmail.com

1. Introduction

This research investigates the power-generating capacity of solar thermoelectric generator-based metal inverted box rib IBR sheeting in a vertical position. IBR sheeting was chosen due to its affordability, availability and profile dimensions which best suits the size of the Peltier tiles used in the investigation. IBR sheeting has an angular trapezoidal profile with large channels (Roof Source, 2017).

Thermoelectric generators (TEGs) convert thermal energy into electrical energy, and are solid-state devices that consist of thermocouples, connected electrically in series, within a thermoelectric module (TEM). These thermoelectric materials convert temperature gradients supplied by a heat source and a heat sink into electrical energy (Fernández-Yáñez et al., 2021). TEMs have a 'hot side' (T_h), which receives the heat and is maintained at a higher temperature, and a 'cold side' (T_c), which is relatively cooler (Hewawasam et al., 2020). The thermocouple in the TEM consists of two dissimilar materials, P and N type, joined electrically in series and thermally in parallel (Cao et al., 2018). TEMs adopt a working principle called the Seebeck effect. This is a phenomenon by which the imposition of a temperature difference between two different electrical conductors produces a voltage (Jaziri et al., 2020). TEMs have received great attention over recent decades due to their ability to convert thermal energy directly into electrical energy, while having no moving parts, no noise, having a scalability, high reliability, long lifespan, and high flexibility in applications, while requiring minimal maintenance, and being compatible with environmental concerns (Hewawasam et al., 2020).

While the power output per TEM is small in magnitude, the proposed configuration lends itself to the coupling of multiple units to increase power output. The current work shows potential for the use of TEGs in this application. Through further investigation, refinement and cost analysis, the system may prove to be a practical method of harvesting solar energy.

One potential application would be to locate a TEG on the side of a large warehouse in a hot climate. The system aims to generate power while keeping the assembly and construction of the system simple, practical, and minimalistic. Outdoor experiments were conducted to determine the temperatures and the resultant temperature gradients the configuration may experience in operation. The data collected established parameters for the laboratory experimental setup. The experiments characterised the power output of the units. The effect of the colour of the metal sheeting and of the electrical connection and arrangements for maximum power output were investigated. For comparative purposes, some variables were removed, which allowed for the testing variable, i.e., the variable being investigated, to be the only variable being tested. Some environmental variables were removed by testing in a laboratory. The TEG was tested in a laboratory, positioned vertically, devoid of most thermal variables, so the results do not reflect those that would be obtained in various potential applications. Galvanised metal, white, and black were chosen as the test colours because the proposed research may have a possible application of generating power on the sheeting of large warehouses. These warehouses are either galvanised or painted white to help cool the warehouse. The colour black was introduced to test whether coating the sheeting black would enhance the power output. Applications of different orientations and geographical locations would require further investigation.

The IV curve generation method (explained in section 3.1 below) is used to read the parameters that are required to calculate Pmax. The effects of the following variables on Pmax are investigated:

i. The effect of roof sheeting colours on power output (galvanised metal, black and white).
ii. Scalability in series vs parallel electrical arrangement for optimum power output.

The work presented is a unique, preliminary and experimental investigation in a potential application of TEGs on standard roof sheeting, together with a proposed method of attaching the TEG system onto roof sheeting. Solar experiments were run, together with laboratory experiments, and the resultant power outputs are discussed and presented.

2. Literature review

Some TEG experimentation, such as in thermoelectric wearable applications, resulted in a low power output range of 0.5-5 mW. These shirts integrated with TEGs serve as a reliable power supply for wearable electronics of low-power requirement (Leonov, 2013; Leonov et al., 2010).

Lashin et al. (2020) designed and tested a TEG system using a partial illumination technique. The performance of the TEG was tested under partial illumination with different percentages of illumination covering, as well as various light intensities (concentrated light produced by a Xenon-Lamp solar simulator with 12× and 105× intensities). The highest power was also found to be generated under the highest light intensity. A similar approach was used in the proposed work, whereby the light intensity is controlled by varying the distance between the lamp and the TEG system.

The power output was measured by Lashin et al. (2020) using a method called the 'IV curve generation method'. The proposed research has adopted the same approach to measure the required parameters for the calculation of the maximum power generated. Therefore, the Pmax found experimentally

in the presented work was established using this power modelling method and is further elaborated on in Section 3.1. Lashin et al. utilised a heat sink in contact with water as a cooling agent, whereas the proposed design will use a more practical and simple solution as the cooling agent: i.e., natural convection occurring on a vertical plate attached to an aluminium heat sink. Lashin et al. tested on a sample with the same number of junctions as used in the experiments in this research.

The electrical arrangement of TEMs was investigated experimentally in various applications (Aranguren et al., 2017, Chen et al., 2012, Dai et al., 2011, Morais et al., 2020, Jeyashree et al., 2020). When using 40 commercially available TEMs, electrical heaters as the heat source with a power rating of 2500 W in total, and a data acquisition system to measure the temperature and voltage, an ensemble provided the required 120 W to power four LEDs. Eight TEMs were connected in series, and this was replicated into five groups, electrically connected in a parallel arrangement (Jaziri et al., 2020). Another set of experiments was conducted in harvesting waste heat via thermoelectric generation. The TEG system used, comprised 32 TEMs suited for high heat applications. The testing utilised thermocouple-type temperature sensors at different locations on the system to monitor temperature fluctuations. A similar approach to measure the temperature gradients using temperature sensors was followed in this work. To investigate the maximum output power, two ammeters and two voltmeters were utilised to measure the current and voltage deviations by applying variable resistances (Aranguren et al., 2017). Similarly, the presented work utilises two ammeters and two voltmeters to measure and monitor the current and voltages generated.

Chen et al. (2012) conducted experiments with four TEMs containing 127 thermoelectric couples of the same size, connected in series to test output power generation. It was found that the higher the number of TEMs connected in series, the higher the maximum power obtained.

Morais et al. (2020) presented an electronic circuit designed to measure the maximum power harvested by utilising low-voltage TEGs. A precise yet low temperature gradient was applied between the hot and cold sides under different TEG configurations, and copper heat sinks were used. It was found that for a high ΔT, the output power measured directly at the output terminals was higher when TEGs were connected in series than when the same TEGs were electrically connected in parallel.

Solar thermoelectric generators (STEGs) are TEGs whose source of heat is the sun. Their main advantage, aside from their 'green' nature, is that they can utilise the entire solar spectrum in contrast to photovoltaics that utilise limited wavelengths of the spectrum (Kraemer et al., 2011). Work has been done on making STEGs as efficient as possible by integrating TEGs in a vacuum plate, thus eliminating heat loss (Kraemer et al., 2011; Lv et al., 2019).

Concentrated solar thermoelectric generators (CSTEGs) are STEGs with an enhanced feature that concentrates the heat onto the hot side where the incident solar flux heating the absorber can be controlled or varied to increase efficiency by encompassing parabolic troughs, parabolic dishes, or optical lenses (Sundarraj et al., 2014). Additionally, due to delayed thermal response, CSTEGs can continue to generate power even if clouds partially block out the sun (Sun et al., 2017). CSTEGs have paved the way for record-breaking efficiencies of TEGs by combining methods of thermal and optical concentration (Cheruvu et al., 2018; Kraemer et al., 2016).

Another CSTEG design set up on a TEG with aluminium fins on the cool side was designed and experimented with by Jeyashree et al. (2020), who also investigated the temperature gradient (ΔT) established by a TEM under the sun. During the day, a maximum ΔT of 96°C, a maximum current of 84.9 mA and 0.65 V was generated from a single TEG. An estimate combination size of 44 TEGs in series and 66 in parallel to power up a 70 W rating LED streetlight was also established. The device used multimeters, thermocouples, and a temperature-monitoring system to explore the parameters mentioned. Jeyashree et al. (2020) monitored the hot side temperature, cold side temperature and the resultant ΔT generated under the sun and displayed the results in a graph. The proposed work adopted a similar ΔT generation strategy. It entailed an electronic temperature-monitoring system made of an Arduino, LCD screen and temperature sensors to achieve realistic data of ΔT readings achieved outdoors, over a span of 150 minutes.

In summary, it may be seen that TEGs are indeed a potential method for harvesting energy. Literature that explored and investigated TEG parameters such as the investigation of ΔT readings achieved, the electrical arrangements of TEGs for required power output, the components utilised in the system during experimentation, and research methodologies adopted was discussed. While the power output per TEG tile is small in magnitude, further advancements in TEG technology may allow for higher efficiency and hence a better power output.

3. Data and methods

3.1 IV curve generation method

The methodology adapted in this research consists of three phases of experimentation. The power modelling method to calculate maximum power experimentally was adopted from Lashin et al. (2020). For the purposes of this research, the IV curve generation method was used to establish the parameters

required to calculate Pmax only. The generation of IV curves is beyond the scope of this work. A portion of the method is used as a technique to calculate Pmax, so IV curves are not generated here. The IV curve generation method is the name of the method used to establish certain TEG properties by measuring the short-circuit current, open-circuit voltage, along with the temperature gradient (ΔT) between the hot side (Th) and the cold side (Tc) under two different conditions. Lashin et al. (2020) use these parameters, found experimentally, to generate graphs containing the current (I) and voltage (V) readings on IV curves. The conditions, shown in Figure 1, are when the circuit terminals are (1) electrically open, and (2) electrically shorted. The heat flow (Qin), and thus, the ΔT was controlled and kept constant under both conditions by using a solar simulator.

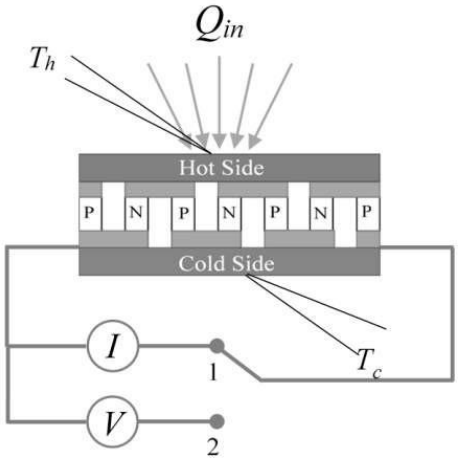

Figure 1: The circuit connection used in the IV curve generation method (Lashin et al., 2020)

The maximum power is given as a function of open circuit voltage and short circuit current in Equation 1 (Lashin et al., 2020).

$$Pmax = \frac{1}{4} Is \times Vo \quad (1)$$

where Pmax is the maximum power generated by the TEG system, Is is the current measured in closed circuit position (A) and Vo is the open circuit voltage measured (V).

The method to establish the above currents and voltages under the two electrical conditions mentioned were found using the TEG performance IV curve generation method of McCarty and Piper (2015), which was also applied by Lashin et al. (2020). This is the scientific backing for the method used to calculate Pmax (Equation 1) from experiments. Further information on the methodology and basis of the method may be found in Lashin et al. (2020) and McCarty and Piper (2015). A summary of this method is given in Table 1, which entails connecting the circuit shown in Figure 1 and running the experiment to obtain four pairs of data points.

Pmax is then calculated using Equation 1, and these results can graphically display the maximum power output under different conditions. The effect of the two parameters on Pmax tested and investigated in this research are discussed in Section 4.

3.2 Components selection and experimental set-up

In this section, the choice of components, material selection and a breakdown of the experimental set-up is elaborated on.

3.2.1 Light source

A commercially available 500 W Eurolux flood lamp was utilised as the light source for the indoor experiments.

3.2.2 Testing jig and inverted box rib sheeting in the TEG system

Figure 2 shows the aluminium L-bars, placed back-to-back, which are used as the heat sink in this design.

Table 1: The summarised steps in the IV curve generation method.

	Circuit condition in Fig. 1	*Points to be measured*
Step 1	Position 1	a) I_s is measured after the desired ΔT is reached b) Initial voltage is observed to be 0V and then V_s c) is measured
Step 2	Position 2	d) V_{s-o} is measured promptly after opening the circuit e) I_{s-o} is measured and the current is observed to then fall to 0A
Step 3	Still in position 2	f) Desired ΔT from step (a) is established, V_o is measured g) Initial current is seen as 0A and the resulting I_o h) is measured
Step 4	Returns to position 1	i) I_{o-s} is measured immediately as the switch is closed j) V_{o-s} is measured immediately as the switch is closed

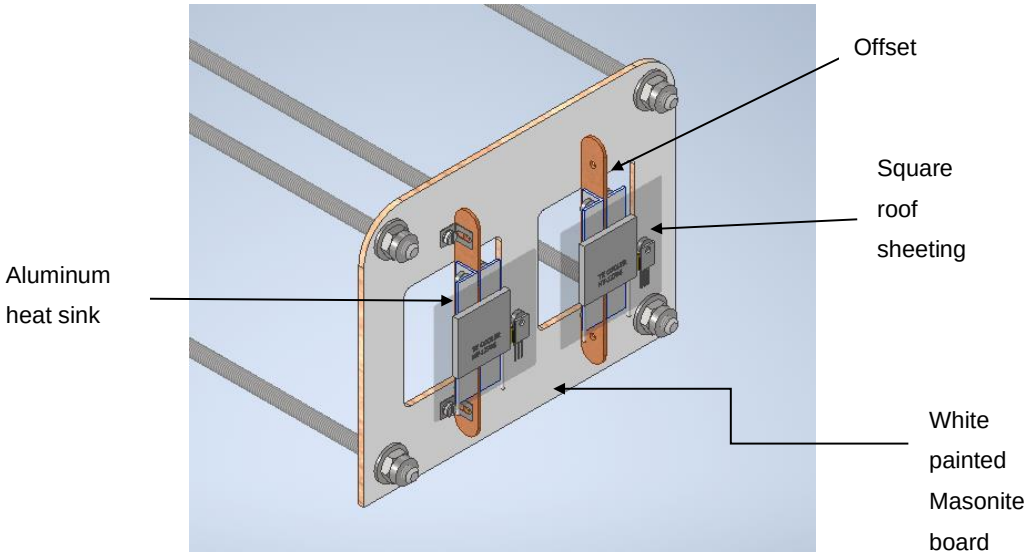

Figure 2: An isometric view of the TEG system jig and coupled components.

It is light-weight, non-magnetic, cost-effective and the good thermal-conductive nature makes it ideal for this application (Radian Thermal, 2024). For these purposes, aluminium heat sinks are widely used and easily available. Aluminium L-type profile angle bars were used in this investigation, which are readily available and of a standard off-the-shelf range. The shape of the L-bars makes them an ideal fit for this configuration as it allows for the bars to be placed back-to-back and for magnets to hold them securely onto the off-set. More magnets can be used to hold these heat sinks against the roof sheeting, with the TEM sandwiched between them. This allows for the 'hot side' of the TEM to be positioned flush against the IBR sheeting and the 'cool side' of the TEM to be positioned against the heat sinks. The length of the heat sinks is the exact length of the IBR sheeting.

It was vital to make certain that the heat received on the hot side of the sheets does not transfer through any holes and mechanical fasteners to the cool side. Using magnets would not require drilling holes through the heat sinks or the sheets, heat will not be conducted via any metal bolts, nuts, or rivets, over to the cool side. Therefore, magnets were used to secure the heat sinks onto the off sets and sheets. Furthermore, the lack of holes and mechanical fasteners in the surface area of the sheets exposed to the sun prevents any effect on the scalability function of the design. Magnets are also simple to use and easy to position. Magnets were also used to position the temperature sensors onto the roof sheeting and heatsink quickly and easily.

Four magnets were used to position the four temperature sensors and 16 (double magnets placed on each end of the L-bar) were used to place the L-bar heat sinks onto the offset (back-to-back) and simultaneously hold the TEM sandwiched between the heat sinks and roof sheeting.

Wooden sticks served as the offset for the TEGs. Wood was chosen for its relatively high insulating properties, which would remove the possibility of any major unwanted heating. Figure 2 presents the CAD isometric view of the masonite board, together with the offsets, heatsinks and TEMs. The IBR sheeting is made transparent to allow viewing of the parts.

3.2.3 Microcontroller and temperature sensors

A programmable microcontroller was required to measure and display the temperatures of the TEG system. Arduino UNO was chosen, due to its numerous advantages such as its user-friendly nature, cost effectiveness, flexibility, and as an opensource electronics platform with extensible software and hardware.

The Arduino was connected and coded to read temperatures measured by four temperature sensors. These readings were displayed on the 16×2 liquid crystal display (LCD) screen. A 16×2 LCD provides 16 columns and two rows of characters, which is ideal to display readings for T1, T2, T3 and T4. T1 and T2 are coded to be displayed one below the other and the same is done for T3 and T4.

LM35DT temperature sensors were chosen, as they have a flat metal head which could be easily sandwiched between the roof sheeting and magnets for ease of application and cost-effectiveness. The LM35DT working temperature range of ±0°C-100°C also suits the temperature requirements of the application. Figure 3 shows the connections of the Arduino microcontroller, temperature sensors and LCD screen.

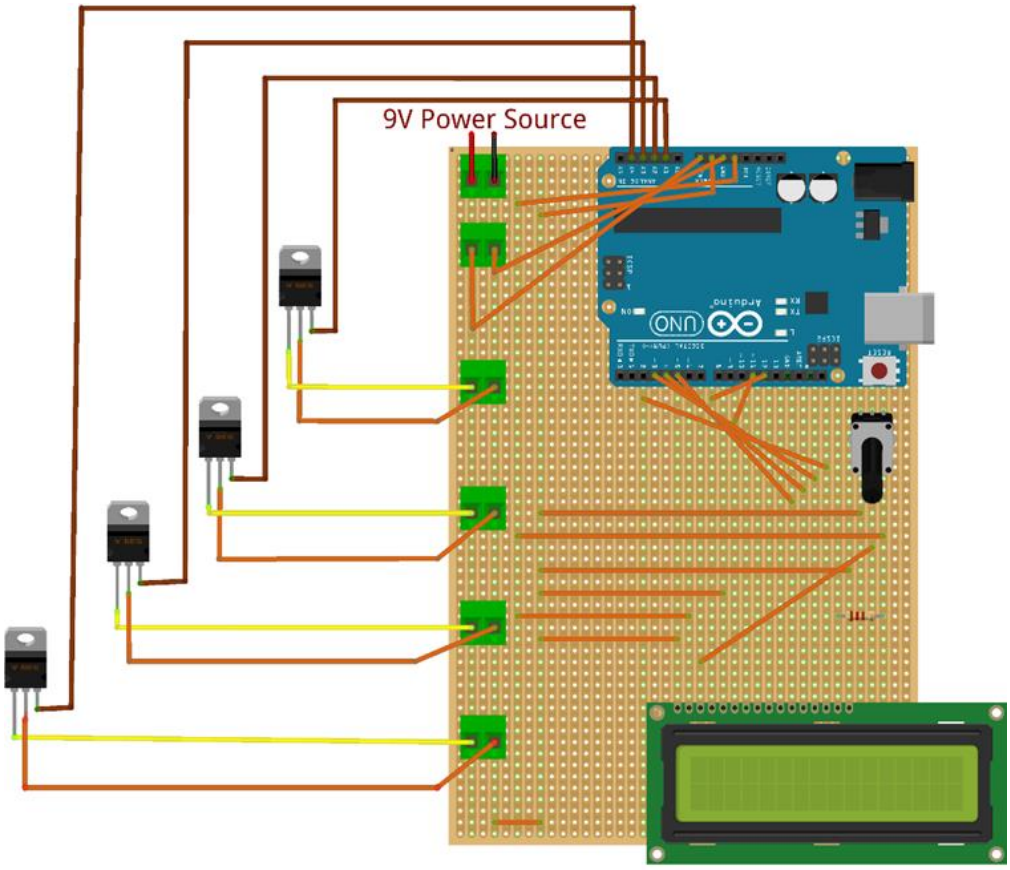

Figure 3: Arduino with temperature sensors for temperature display.

3.2.4 Circuit with switch and four digital multimeters

The stripboard with terminals for connection of the TEMs, multimeters leads, and switches was used as a base for the required circuit. The two switches and eight two-way terminals were soldered onto the stripboard.

A TEM can be connected onto another stripboard (SB2) as a unit. For the unit configuration, a toggle switch is needed. SB2 has four plastic spaces drilled onto the reverse side to prevent electrical interference when placed on a surface during experimentation. Figure 4 shows the circuit diagram connected onto SB2 as a unit.

However, for the series and parallel arrangements of TEMs, the circuits displayed in Figures 5 and 6 were wired and connected using 0.34mm solid wire, terminal blocks for nodes, alligator clips and a large push-button switch. Four UNI-T UT33+ series palm-size digital multimeters were used to measure voltage and current readings generated by the TEG.

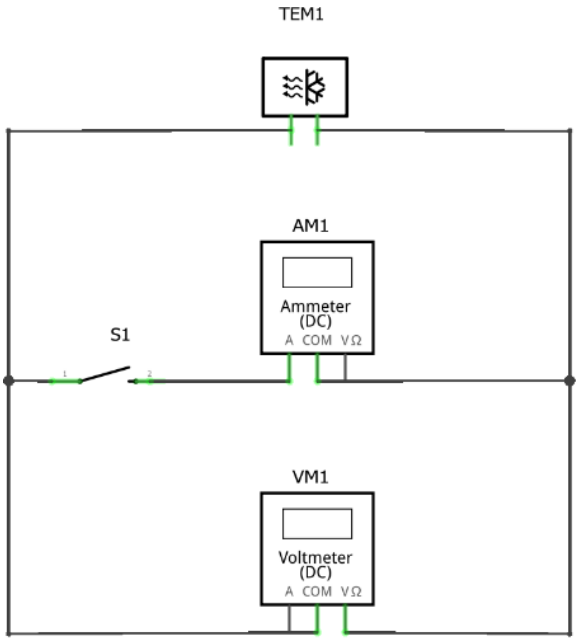

Figure 4: Circuit diagram for SB2 when a thermoelectric module is connected as a unit.

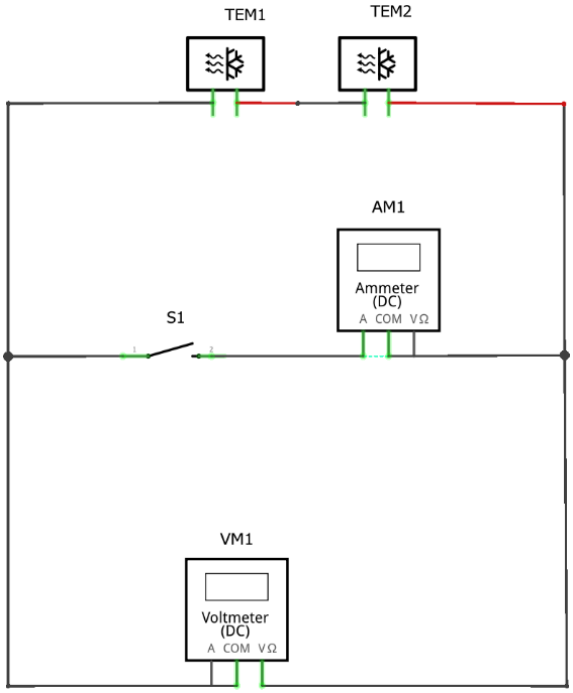

Figure 5: Circuit diagram for SB2 when two thermoelectric modules are connected in series.

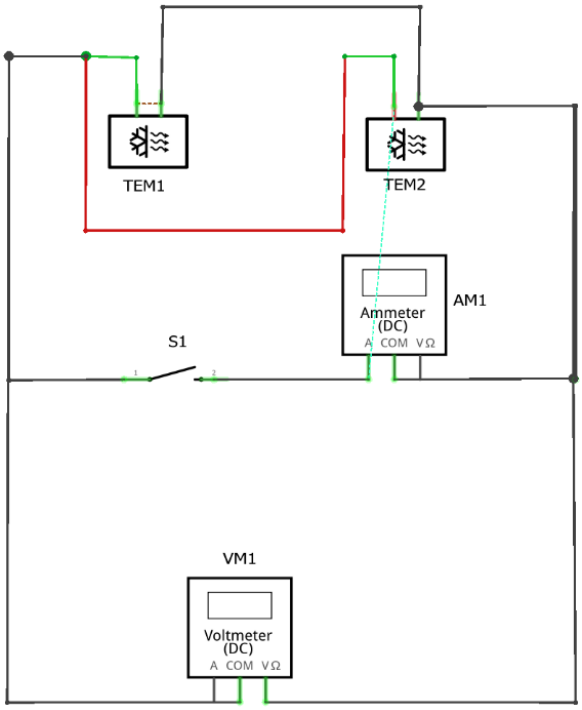

Figure 6: Circuit diagram for SB2 when two thermoelectric modules are connected in parallel.

3.2.5 TEG1 and TEG2

Each TEG ensemble is comprised of the roof sheet, a TEM, two aluminium L-bar rods faced back-to-back to form a heatsink, two temperature sensors connected to SB1, and the required number of digital multimeters (depending on the electrical configuration of the TEMs) connected on SB2. Both TEGs are exactly the same and run simultaneously under the same conditions. When unit configuration experiments are run, TEG1 is used in the set-up.

3.3 Testing and experiments.

This section elaborates on the steps taken in the testing, the methodology, the expected outcomes, and the breakdown of experimental phases in the investigation.

3.3.1 Phase 1: Colour- and distance-varied indoor experiments.

Phase 1 entails running a series of nine indoor experiments. The galvanised roof sheeting was exposed to the heat source at three distances: 300 mm, 600 mm and 900 mm. The experiments at different distances were repeated for the remaining colours of roof sheeting. The four steps of the IV curve generation method were carried out.

The data was continuously acquired. In addition to the data achieved by this method, the corresponding ΔT values were also video-recorded, and the generated parameter readings were logged manually. The output power generated during each switch was calculated on a spreadsheet in Microsoft Excel. The effect of distance (between the heat source and the TEG system), and the effect of the three colour sheets on the output power generated by the system was then analysed. Figure 7 is a photograph of the TEG system with black-coated roof sheets, in closed circuit position, during experiments at 600 mm. The summary of experiments run in phase 1 is given in Table 2.

3.3.2 Phase 2: Outdoor conditions

For phase 2, to achieve realistic data on the expected ΔT range in the sun, the experiment of black sheets outdoors when exposed to sunlight was run. The same experiment set-up which was used in phase 1 was then shifted outside, under the sun. The resulting ΔT readings over a span of 150 minutes was acquired. The summary of experiments run in phase 2 is given in Table 3.

Table 2: Summary of experiments run in phase 1.

Experiment number	*Roof sheeting colour*	*Distance between TEG and lamp(mm)*	*Electrical configuration*	*Outcome parameters*
1	Galvanized	300	Unit	ΔT, V_o, I_s and the resultant P_{max} derived from the TEG
2		600		
3		900		
4	Black	300	Unit	
5		600		
6		900		
7	White	300		
8		600	Unit	
9		900		

Figure 7: The thermoelectric generator system with black-coated roof sheets in closed circuit position during experiments at 600 mm.

Table 3: Summary of experiments run in phase 2.

Experiment no.	*Roof sheeting colour*	*Electrical configuration*	*Outcome parameters*
1	Black	Unit	T_h, T_c and ΔT achieved by the TEG over a span of 150 minutes

3.3.3 Phase 3: TEM arrangement for maximum power output and scalability.

TEG performance is derived empirically, so it was necessary to test and investigate which configuration works best. The performance curves provided by the manufacturer of the TEM do not provide design equations. This is because TEGs are an innovative and relatively new field of research and constantly evolving (Leonov et al., 2010). Furthermore, the common applications of TEM involve applying a power to the TEM, which in turn allows for the TEM to be used in heating or cooling applications. However, this experiment tested the TEM for power generation by applying a temperature gradient and investigating the resultant power generated.

In phase 3, the TEG was then set up using the colour sheet that performed best i.e., generated the highest Pmax. The TEM was connected electrically as a unit and was run indoors at the three distance variations, i.e., 300 mm, 600 mm and 900 mm. The same was done for the remaining two arrangements, i.e., two TEMs electrically connected in series and then two TEMs electrically connected in parallel.

Table 4: Summary of experiments run in phase 3.

Experiment number	*Roof sheeting colour*	*Distance between TEG and lamp(mm)*	*Electrical configuration*	*Outcome parameters*
1	Black	300	Unit	ΔT, V_o, I_s and the resultant P_{max} derived by the TEG.
2		600		
3		900		
4	Black	300	Series	
5		600		
6		900		
7	Black	300	Parallel	
8		600		
9		900		

The resulting power output from each distance and configuration was studied, compared, and analysed. This was done to extract the best possible electrical arrangement of TEGs when scaled-up for maximum power generation.

The results from this experiment can also predict the expected output solar power generated when electrically connected in the 'ideal' electrical arrangement for maximum power output. This is discussed in Section 4.3. For the purpose of future research, the expected solar output power when the system is scaled-up could also be predicted and compared to the output power generated by PV solar panels of the same scale. The summary of experiments run in phase 3 is given in Table 4.

4. Results and findings

This section presents a summary of the results and findings in the context of this investigation.

4.1 Phase 1: Colour- and distance-varied indoor experiments

Figure 8 displays the Pmax vs ΔT data acquired from phase 1 of the experiments as a bar graph. The colour and distance variations have been shown on the x axis as follows:

- G300 – galvanised sheet at 300 mm from the heat source.
- G600 – galvanised sheet at 600 mm from the heat source.
- G900 – galvanised sheet at 900 mm from the heat source.
- W300 – white coated sheet at 300 mm from the heat source.
- W600 – white-coated sheet at 600 mm from the heat source.
- W900 – white-coated sheet at 900 mm from the heat source.
- B300 – black-coated sheet at 300 mm from the heat source.
- B600 – black-coated sheet at 600 mm from the heat source.
- B900 – black-coated sheet at 900mm from the heat source.

The dual y-axes display the-corresponding Pmax values of the blue bars on the left-hand side, and the corresponding ΔT values of the orange bars on the right-hand side. Pmax and ΔT is measured in milliwatts (μW) and degrees Celsius (°C) respectively. The TEG1 experiment-consists of 10 data sets per switch (derived from the IV curve generation method) that were averaged into a data pair (ΔT and-corresponding Pmax) for each-colour/distance experiment shown on the x axis.

The primary outcome from phase 1 is that the black-coated sheets of TEG1 outperformed all other sheet-colours. The black sheets positioned at all three distances had a higher output ΔT and resultant Pmax than the comparative galvanized and white-coated sheets at the same distances. The black sheets' performance was then followed by galvanized and then white-coated sheets. It is noteworthy that the galvanised sheets outperformed the white sheets. It can be concluded that if this TEG is applied to the warehouse roofing or wall cladding, optimum output may be achieved by coating the roof sheeting with a matte black paint.

4.1 Phase 2 – Outdoor conditions.

Figure 9 displays the Th, Tc and ΔT solar data acquired from phase 2 of experiments as three-line graphs on the same axes. A black-coated IBR sheet was used in this experiment, since the black-coated sheets achieved the highest output in phase 1. The x axis displays the time lapse in minutes over a span of 150 minutes and the y axis displays the resultant ΔT generated by the TEG in the sun. The solar experimental data displayed in the graph outlines the TEG's characteristic behaviour in accordance with its temperature parameters throughout the span of 150 minutes on a cool day.

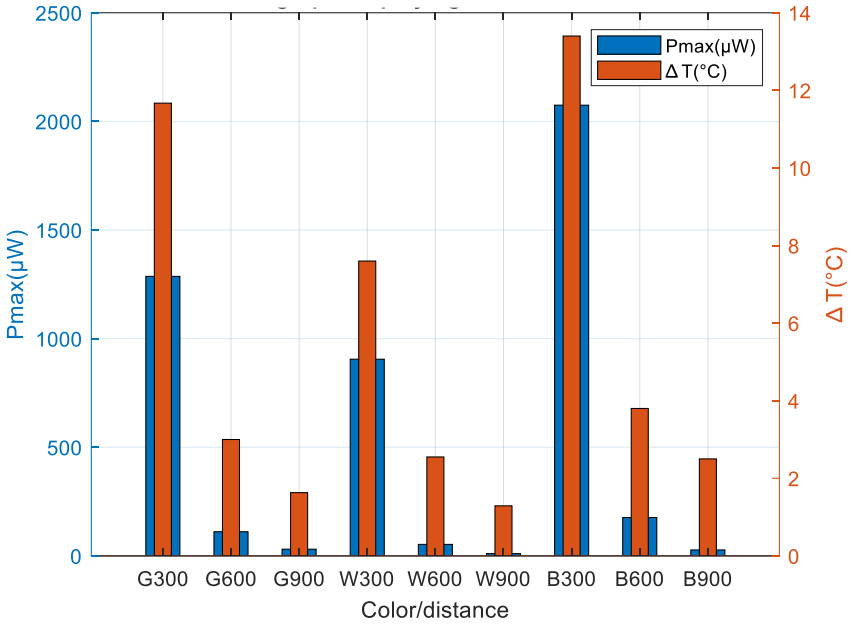

Figure 8: Graph displaying averaged results obtained for the colour- and distance-varied tests.

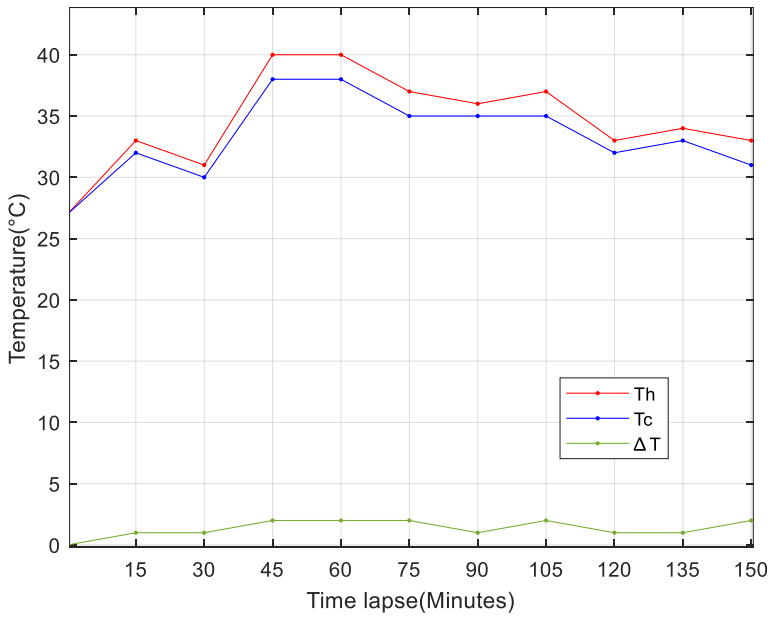

Figure 9: Graph displaying temperature vs time results obtained outdoors on a cool day when the experiment was run for 150 minutes.

Results from phase 2 show that the output ΔT was found to be relatively consistent in a range of 1–2 °C in the experiment, so it may be deduced that the aluminium L-bars perform well as heat sinks. An average T_h, T_c and ΔT over a span of 150 minutes of 34.55 °C, 33.19 °C, and 1.35 °C was established in the sun on a cool day, respectively.

4.3 Phase 3: TEM arrangement for maximum power output and scalability

It was found from phase 1 that the black-coated sheets greatly enhanced the TEG output. Therefore, the experimental set up for phase 3 utilised black sheets to test for the 'ideal' electrical arrangement of TEGs for maximum output.

Figure 10 displays the acquired data from phase 3, stabilised, as a bar graph. The configuration and distance variations are displayed on the x axis as the following labels:

- U900 – TEG as a unit, set 900 mm away from the heat source.
- U600 – TEG as a unit, set 600 mm away from the heat source.

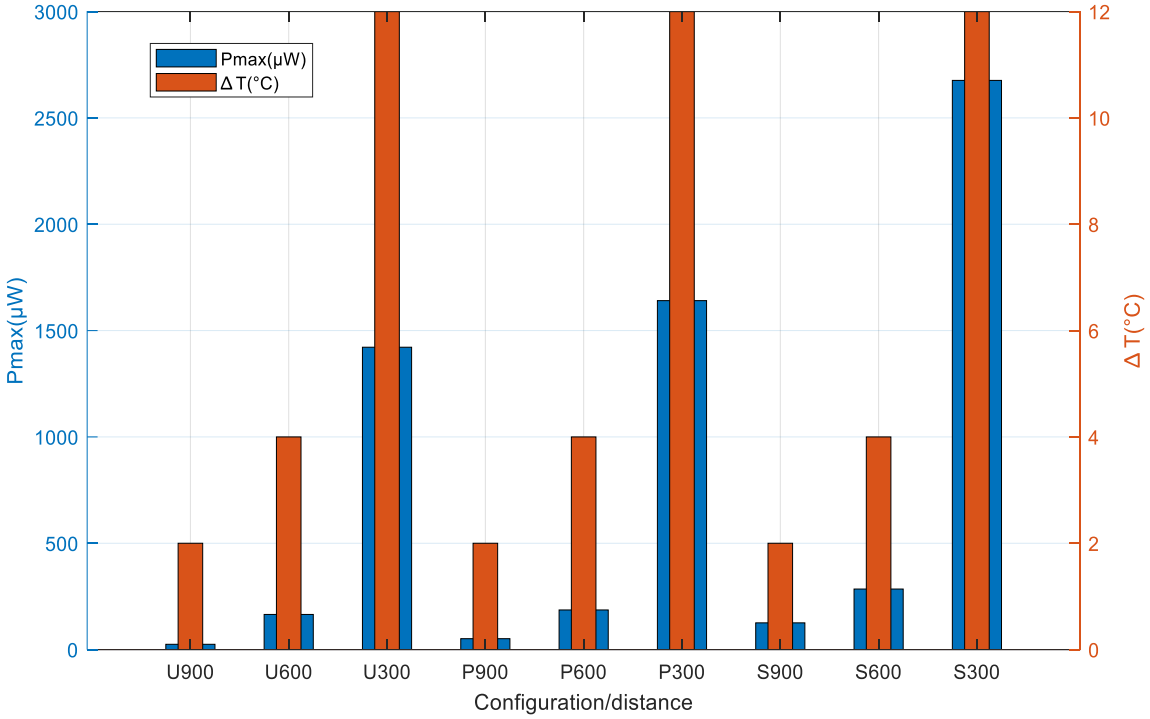

Figure 10: Bar graph displaying averaged results, once readings were stabilised, for the different configurations and distances for black sheets.

- U300 – TEG as a unit, set 300 mm away from the heat source.
- P900 – two TEGs connected in parallel at 900 mm from the heat source.
- P600 – two TEGs connected in parallel at 600 mm from the heat source.
- P300 – two TEGs are connected in parallel at 300 mm from the heat source.
- S900 – two TEGs are connected in series at 900 mm from the heat source.
- S600 – two TEGs are connected in series at 600 mm from the heat source.
- S300 – two TEGs are connected in series at 300 mm from the heat source.

The dual y-axes display the corresponding Pmax values of the blue bars on the left-hand-side y axis and the corresponding ΔT values of the orange bars on the right-hand-side y axis. Pmax and ΔT are measured in microwatts (μW) and degrees Celsius (°C) respectively.

The data acquired from phase 3 was then plotted as points on axes in Figure 11. In Figure 11, the Pmax values displayed on the y axis and the ΔT values displayed on the x axis, are measured in microwatts (μW) and degrees Celsius (°C), respectively. The data acquired from the unit, parallel and series electrical configuration is indicated by red dots, green crosses, and blue squares respectively.

If Figures 10 and 11 are cross-checked, it is evident that the TEG in series configuration generated the highest Pmax when located 300 mm from the heat source, followed by 600 mm and 900 mm. The same pattern is found for the unit and parallel configurations. This accords with the findings of Lashin et al. (2020) (see section 2) established: i.e., the highest intensity of heat will generate the highest power output.

The data shows that the TEG system, when placed 900 mm from the heat source, experiences a ΔT of 2 °C. This is doubled at 600 mm and increases sixfold when positioned at 300 mm.

Similarly, when placed at 900 mm from the heat source, the TEG system as a unit configuration, generates a Pmax of 24.89 μW. This is doubled when connected in parallel and increases fivefold when in a series arrangement.

When the TEG system is placed at 600 mm, a Pmax of 165.23 μW is generated by the unit configuration. This increases by a factor of 1.12 when connected in parallel and by a factor of 1.72 when connected in series.

For 300 mm placement, the TEG system generates a Pmax of 1421.74 μW as a unit. This increases by a factor of 1.15 when connected in parallel and by a factor of 1.88 times when connected in series.

The analysis of phase 3 data acquisition is summarised in Table 5.

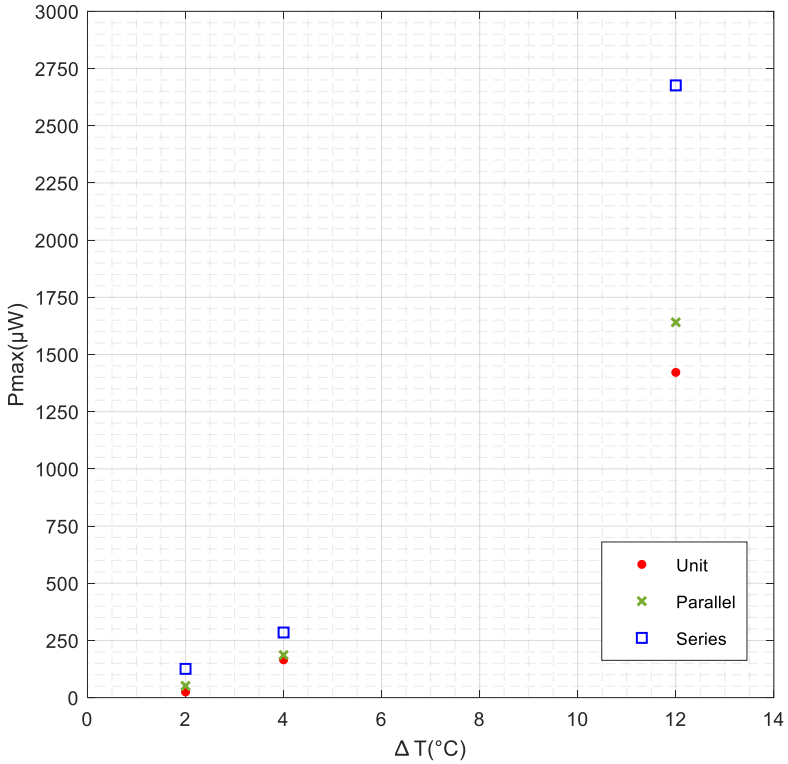

Figure 11: Plot displaying averaged results once readings were stabilised, for the different configurations, colours, and distances.

Table 5: Results from phase 3 of the experiment.

Distance(mm)	*Parameter*	*Electrical connection*	*Factor of increase*
900	ΔT	Unit, parallel and series	0
600			2
300			6
900	Pmax	Unit	0
		Parallel	2
		Series	5
600	Pmax	Unit	0
		Parallel	1.12
		Series	1.72
300	Pmax	Unit	0
		Parallel	1.15
		Series	1.88

5. Conclusion

The research investigated the effect that two variables have on power output of a TEG system coupled with IBR sheeting. There was no testing of applications, but a potential application, requiring further research, may be on the surface areas of large warehouses. A modular prototype was configured, relevant tests were run, and the performance characteristics obtained from experiments were discussed.

The TEG was tested in a vertical position to allow for natural convection, and devoid of most other thermal variables, so it may not reflect results that would be obtained in real applications. The TEG prototype was exposed to the light source at different distances, perpendicular to the sheets. The study investigated the effect that the two variables have on the amount of solar power harvested – i.e., the colour of metal IBR sheeting, and the ideal electrical

arrangement for scalability of Peltier tiles for maximum power output.

The primary outcome is that the black-coated sheets of TEG1 outperformed the other two colours. It can be concluded that if this TEG system is applied to warehouse side sheeting and wall cladding, an optimum output may be established by coating the sheeting with a matte black paint. The output ΔT from solar experiments was found to be of a consistent range, showing that the aluminium L-bars perform well as heat sinks and fulfilled their purpose of regulating ΔT. It is also concluded that the TEGs in series configuration, generated the highest Pmax when located closest to the light source.

As discussed, the highest Pmax generated by a unit TEM in this experiment was 1421.74 μW. This Pmax was established by the 40×40 mm TEM in the TEG system. For normalising purposes, it can be extrapolated that, on a surface area of one square metre, 625 TEMs as units are required and may generate a Pmax of 0.89 W/m^2. The TEG system may generate 0.89 W/m^2 on black-coated IBR sheeting. It is acknowledged that the power output is low, and some applications may be low-power wearables, power storage in batteries for later use, or low-power lighting. It may be concluded that TEGs could be a reasonable method for harvesting solar energy on IBR sheeting, specifically in a vertical position.

TEG devices may improve in efficiency through future technological advancements giving improved power output. The scalability option could generate more energy on large surface areas, making the system potentially useful in warehouses, when the warehouse sheeting is painted matte black.

The results merit further investigation and refinement into the use of TEGs on IBR sheeting where a TEG system like that in the experiment may be set up in a user-friendly, simple, cost-effective and practical manner for harvesting solar energy.

References

Aranguren, P., Araiz, M., Astrain, D. and Martínez, A., 2017. Thermoelectric generators for waste heat harvesting: A computational and experimental approach. *Energy Conversion and Management*, 148: 680-691.

Cao, Q., Luan, W. and Wang, T., 2018. Performance enhancement of heat pipes assisted thermoelectric generator for automobile exhaust heat recovery. *Applied Thermal Engineering*, 130: 1472-1479.

Chen, W.H., Liao, C.Y., Hung, C.I. and Huang, W.L., 2012. Experimental study on thermoelectric modules for power generation at various operating conditions. *Energy,* 45(1): 874-881.

Cheruvu, P., Kumar, V.P. and Barshilia, H.C., 2018. Experimental analysis and evaluation of a vacuum enclosed concentrated solar thermoelectric generator coupled with a spectrally selective absorber coating. *International Journal of Sustainable Energy,* 37(8): 782-798.

Dai, D., Zhou, Y. and Liu, J., 2011. Liquid metal based thermoelectric generation system for waste heat recovery. *Renewable Energy,* 36(12): 3530-3536.

Fernández-Yáñez, P., Romero, V., Armas, O. and Cerretti, G., 2021. Thermal management of thermoelectric generators for waste energy recovery. *Applied Thermal Engineering,* 196, p.117291.

Hewawasam, L.S., Jayasena, A.S., Afnan, M.M.M., Ranasinghe, R.A.C.P. and Wijewardane, M.A., 2020. Waste heat recovery from thermo-electric generators (TEGs). *Energy Reports*, 6: 474-479.

Jaziri, N., Boughamoura, A., Müller, J., Mezghani, B., Tounsi, F. and Ismail, M., 2020. A comprehensive review of thermoelectric generators: Technologies and common applications. *Energy Reports*, 6: 264-287.

Jeyashree, Y., Sukhi, Y., Juliet, A.V., Jame, S.L. and Indirani, S., 2020. Concentrated solar thermal energy harvesting using Bi2Te3based thermoelectric generator. *Materials Science in Semiconductor Processing*, 107, p.104782.

Kraemer, D., Jie, Q., McEnaney, K., Cao, F., Liu, W., Weinstein, L.A., Loomis, J., Ren, Z. and Chen, G., 2016. Concentrating solar thermoelectric generators with a peak efficiency of 7.4%. N*ature Energy*, 1(11): 1-8.

Lashin, A., Al Turkestani, M. and Sabry, M., 2020. Performance of a thermoelectric generator partially illuminated with highly concentrated light. *Energies*, 13(14), p.3627

Leonov, V., 2013. Thermoelectric energy harvesting of human body heat for wearable sensors. *IEEE Sensors Journal,* 13(6): 2284-2291.

Leonov, V., Torfs, T., Vullers, R.J. and Van Hoof, C., 2010. Hybrid thermoelectric–photovoltaic generators in wireless electroencephalography diadem and electrocardiography shirt. *Journal of Electronic Materials,* 39: 1674-1680.

Lv, S., He, W., Hu, Z., Liu, M., Qin, M., Shen, S. and Gong, W., 2019. High-performance terrestrial solar thermoelectric generators without optical concentration for residential and commercial rooftops. *Energy Conversion and Management,* 196: 69-76.

McCarty, R. and Piper, R., 2015. Voltage–current curves to characterize thermoelectric generators. *Journal of Electronic Materials*, 44: 1896-1901.

Morais, F., Carvalhaes-Dias, P., Duarte, L., Spengler, A., de Paiva, K., Martins, T., Cabot, A. and Siqueira Dias, J., 2020. Optimization of the TEGs configuration (series/parallel) in energy harvesting systems with low-voltage thermoelectric generators connected to ultra-low voltage DC–DC converters. *Energies,* 13(9), p.2297.

Roof Source Pty Ltd. (2017) Roof Sheeting [Online]. Available: https://www.roofsource.co.za/roof-metal-sheeting/ [Accessed 26th September 2022].

Radian Thermal Products. Aluminium heatsink. https://www.radianheatsinks.com/aluminum-heatsink/ [Accessed 22nd September, 2022].

Sun, D., Shen, L., Yao, Y., Chen, H., Jin, S. and He, H., 2017. The real-time study of solar thermoelectric generator. *Applied Thermal Engineering*, 119: 347-359.

Sundarraj, P., Maity, D., Roy, S.S. and Taylor, R.A., 2014. Recent advances in thermoelectric materials and solar thermoelectric generators–a critical review. *RSC Advances,* 4(87): 46860-46874.